

# Advanced VIRGO: detector optimization for gravitational waves by inspiralling binaries

ALESSANDRO D.A.M. SPALLICCI<sup>1\*</sup>, SOFIANE AODIA<sup>1,2</sup>,

JOSÉ DE FREITAS PACHECO<sup>1</sup>, GIORGIO FROSSATI<sup>3</sup>, TANIA REGIMBAU<sup>4</sup>

<sup>1</sup> Dépt. d'Astrophysique Relativiste ARTEMIS, Observatoire de la Côte d'Azur, Nice

<sup>2</sup> Université de Nice-Sophia Antipolis

<sup>3</sup> Kamerlingh Onnes Laboratorium, Rijksuniversiteit van Leiden

<sup>4</sup> School of Physics and Astronomy, University of Cardiff

Emails: spallicci@obs-nice.fr, aodia@obs-nice.fr, pacheco@obs-nice.fr

frossati@physics.leidenuniv.nl, tania.regimbau@astro.cf.ac.uk

December 2, 2024

PACS: 95.30.Sf 95.55.Ym 97.60.Jd

## Abstract

An advanced European detector is currently considered. A strong R&D program will be necessary to improve the actual sensitivity of VIRGO and GEO. Naturally such effort must aim to optimize detection, given limited budget and manpower. Among sources, coalescing binaries appear among the most interesting and known. Thus, improvements in signal to noise ratio (S/N) by noise abatement in VIRGO, for inspiralling binaries of small chirp mass, are discussed. VIRGO detection bandwidth is divided into four sub-bands according to the dominant noise (whether seismic, thermal from pendula and mirrors, shot). Firstly, it is identified that mirror thermal noise reduction provides the highest gain increment in S/N. On the assumption that the technological challenges lying ahead, and the relative necessary budgets, are equally relevant in all sub-bands, it is recommended to gear R&D strategies to a future EURO detector operating at cryogenic temperatures. Secondly, the frequency of 50 Hz is identified as the single optimal frequency at which lies the potential largest increment in S/N for VIRGO. Thirdly, enlargement of the bandwidth, where noise is reduced, produces a shift to higher frequency of the optimal frequency (e.g. for 100 Hz band, the optimal frequency is 75 Hz). Fourthly, noise reduction factor and width of band, where such reduction occurs, both concur to S/N improvement and equivalent gains may be achieved, proposing alternative R&D strategies. Finally, on the basis of our recent estimates on coalescing Neutron Stars (NS) binaries rates, the detection rate by the actual VIRGO configuration is about one every 27 years. An improvement in the strain sensitivity of a factor 3 in the mirror thermal noise band, implies a detection rate of about one coalescing NS binary every 5 years, or 4 detection a year for a noise reduction factor of 10.

## 1 Introduction

The motivation of this work is to support the forthcoming R&D effort for the upgrading of VIRGO<sup>1</sup> French-Italian and GEO<sup>2</sup> British-German gravitational waves interferometer. A major concern is how to gear efforts in R&D such that the improvements will sensibly increase the probability of detection. To such end, this note takes a very pragmatic approach. Among sources, scientific interest, knowledge of the model, number of events, all hint to coalescing binaries as primary candidate for first detection. We therefore analyze in which part of the interferometer spectrum, noise reduction for achieving the largest increment in signal to noise ratio (S/N) would be optimal.

The structure of the paper is the following. In the second section, we briefly summarize the main expressions

---

\*BP 4229, Boulevard de l'Observatoire, 06304 Nice, France

<sup>1</sup><http://www.virgo.infn.it>

<sup>2</sup><http://www.geo600.uni-hannover.de>

that determine S/N for inspiralling binaries and present the main features of the VIRGO sensitivity curve, limited by various noise sources. In the third section, we perform the analysis leading to our main findings on the relation between noise abatement and the increment in S/N. In the fourth section we describe the main technological challenges facing thermal noise mirror reduction. In the fifth section, we determine detection rates using the results of a recent analysis on event rates mainly performed at our premises. We hint to the impact of the S/N improvement on the explorability of the universe.

## 2 Inspiralling binaries and VIRGO features

Matched filtering is the baseline detection tool, although demanding in terms of filters. It enhances S/N by the square root of the number of observed cycles in the binary. The simplest post-Newtonian model is assumed for our analysis of the relation between VIRGO improved sensitivity curve and S/N. A more accurate model may marginally change the absolute values of S/N but not their relative values we are interested to. Indeed, in this exercise what matters is the relation between technology improvement in this or that frequency band and gain in S/N.

The S/N is given by (Helstrom, 1968):

$$\frac{S}{N} = 2\sqrt{\int_0^\infty \frac{|\tilde{h}|^2}{I(f)} df} \quad (1)$$

where  $\tilde{h}$  is the Fourier transform of the signal and  $I(f)$  is the one-sided spectral density of the noise. A frequently used and approximated expression, derived by the Peters-Mathews model (Peters, 1964; and Mathews, 1963) is given by (Spallicci et al., 1997):

$$\frac{S}{N} = 2\tilde{A}\sqrt{\int_0^\infty \frac{1}{f^{7/3}I(f)} df} \quad (2)$$

where

$$\tilde{A} = \sqrt{\frac{5}{24}} \frac{1}{\pi^{2/3}} \frac{\mathcal{M}^{5/6}}{r} \quad (3)$$

$$\mathcal{M} = (\mu M^{2/3})^{3/5} = \frac{(M_1 M_2)^{3/5}}{(M_1 + M_2)^{1/5}} \quad (4)$$

$\mathcal{M}, \mu, M, M_1, M_2$  being the chirp, reduced, total and single masses of the binary. A factor 2/5 is to be applied to  $\tilde{A}$  for taking into account the average relative orientation between binary and detector. The VIRGO sensitivity curve, *fig. 1*, is given by:

$$I_{old}(f) = 3.8 \times 10^{-51} f^2 + 9.5 \times 10^{-46} + 1.6 \times 10^{-43} f^{-1} + 8.3 \times 10^{-37} f^{-5} \quad (5)$$

The sensitivity curve of VIRGO is divided in the following zones dominated by a specific noise (Punturo, 2003):

- a. 1 - 2.1 Hz seismic noise
- b. 2.1 - 42 Hz thermal pendulum
- c. 42 - 140 Hz thermal mirror
- d. 140 - 10.000 Hz shot noise

## 3 Analysis for an improved S/N

We define the gain simply as (Spallicci, 2003):

$$G = \frac{(S/N)_{new}}{(S/N)_{old}} = \left( \int_{1 \text{ Hz}}^{10 \text{ KHz}} \frac{I_{old}}{I_{new}} df \right)^{1/2} \quad (6)$$

and introduce the noise abatement factor  $k$  such that

$$I_{new} = I_{old} \left\{ \frac{1}{k^2} \left[ u \left( f + \frac{\Delta f}{2} - f_0 \right) - u \left( f - \frac{\Delta f}{2} - f_0 \right) \right] + \left[ 1 - u \left( f + \frac{\Delta f}{2} - f_0 \right) + u \left( f - \frac{\Delta f}{2} - f_0 \right) \right] \right\} \quad (7)$$

where the step function  $u(f)$  is defined of value 1 if  $f > 0$ , 1/2 if  $f = 0$ , 0 if  $f < 0$ . The operator  $k$  acts on a sub-band  $\Delta f$  centered on  $f_0$ . Therefore, the function  $I_{new}$  takes the values  $I_{old}$  or  $I_{old}/k^2$ , outside and within the chosen window<sup>3</sup>.

Our considerations are applicable solely to the inspiralling phase of a coalescing binary. This is equivalent to say that only neutron stars and small black holes of few solar masses are encompassed by this analysis. The contribution to S/N given by final merge and, possibly, quasi-normal ringing is neglected. The latter two phases uniquely characterize massive black holes that would enter the VIRGO band only after the inspiralling.

The first investigation aims to identify the S/N improvement for abatement of the noise in one of the four a-d sub-bands defined in the previous section. We improve each of the four sub-bands in turns; *fig. 2* shows the behavior of S/N gain for different values of noise abatement. It is to be noted that improvement in the (a) sub-band implies also an enlargement of the window, lowering the left extremity point of the sensitivity curve. We observe that abatement in the thermal mirror noise band (c) provides the largest S/N gain.

Instead, *fig. 3* reports the same previous curves, but normalized by the sub-band respective bandwidths. The largest S/N gain per unit frequency is in the (a) sub-band, not reported in *fig. 3* being out of scale, due to a larger observed number of cycles. The advantage of lowering the noise in the very low frequencies is the extremely very narrow band such improvement is to be applied to. The disadvantage is that even one order of magnitude abatement does not improve S/N sensibly. Thus, we observe that the thermal pendulum (b) and mirror bands (c) record the largest *convenient* normalized S/N gains, when their respective noises are reduced.

The second investigation aims to identify the optimal frequency around which the noise abatement should be performed. We firstly look for the single frequency at which noise reduction is more beneficial. We identify 50 Hz (*fig. 4*), the optimal frequency around which noise abatement provides the largest gain in S/N.

Further we analyze where noise reduction in a given bandwidth of 40 or 100 Hz would be more beneficial and *fig.s 5-6* show the behavior of S/N gain for different bandwidths where noise has been reduced. Reducing the noise in the (c) band, the gain  $G$  lies between 2.5 and 8.

Finally, it appears that there are equivalent situations achieving the same gain in S/N, e.g. *fig. 5* and *fig. 6* report a similar gain  $G = 2.5$  for  $k = 3$  at 75 Hz in a bandwidth of 100 Hz or for  $k = 10$  at 15 Hz in a bandwidth of 35 Hz (DC-35 Hz). Incidentally, for signal recycling, there is a similar gain in S/N, 1.5 or 50% for noise abatement factor  $k = 5$  at 200 Hz in a bandwidth of 20 Hz or for  $k = 3$  at 25 Hz in a bandwidth of 40 Hz. Furthermore, the increment of the bandwidth shifts to higher frequency the optimal frequency (e.g. for 100 Hz band, the optimal frequency is 75 Hz).

## 4 Thermal mirror noise

In the 42-140 Hz band, the major limiting factor is coming from the thermal noise of the mirror but a large noise reduction would imply lowering the contributions from the pendulum and the shot noises too. The suspended test masses thermal noise power spectrum is given by:

$$\tilde{x}_m^2(\omega) \simeq \frac{8B_k T}{\omega} \phi_m(\omega) U \quad (8)$$

where  $B_k$  is the Boltzmann constant,  $T$  the temperature,  $U$  the strain energy stored in the substrate subjected to a normalized static pressure having the same (Gaussian) distribution of the laser beam and  $\phi_m$  the loss angle of the mirror, depending upon the strain energy (Harry et al., 2002). The evaluation of the strain energy  $U$ , for

<sup>3</sup> If the central frequency  $f_0$  around which noise is abated is in the lowest part of the spectrum, the bandwidth is not equally wide at both sides of  $f_0$ .

a finite size mirror, has been done by Bondu et al. (1998).

Furthermore, as demonstrated by Braginsky et al. (1998, 2003), the thermo-elastic effect is present both in the mirror and in the coating and it is usually referred as the thermo-dynamical contribution.

The direct temperature dependence of the fluctuation power spectrum suggests that, if we want gain an order of magnitude in terms of the space-time strain  $h$ , we must decrease the temperature of about two orders of magnitude or in other words we must go to cryogenic temperature. Planning entails use of crystalline Silicon to realize the suspension for its lower loss angle  $\phi_m$  than fused silica; its thermal expansion coefficient goes essentially to zero before 10 K. Also, the thermal conductivity of the Silicon increases at low temperature pushing up in frequency the residual thermo-elastic peak. The latter property of Si is also fundamental for its use in an advanced interferometric detector, in which the power circulating is so high that the thermal lensing effect in the mirrors could change the optical properties of the Fabry-Perot cavities, affecting the whole functioning. The Silicon thermo-mechanical properties suggest it as a good candidate also to realize the mirrors in the interferometer. All the thermo-dynamical phenomena related to the substrate will disappear using Silicon mirrors at cryogenic temperatures.

Different is the behavior of the coatings. Recent preliminary measurements showed that the loss angle of  $Ta_2O_5$  coatings doesn't decrease with the temperature. In any case, at least a reduction of a factor 10 due to the direct temperature dependence is expected in terms of noise amplitude spectral density.

Obviously, in order to use Silicon mirrors, it is necessary to change the wavelength of the laser. In fact, Si transmittivity is very poor at the usual  $1.064\mu m$  wavelength used in the current Nd:YAG laser in GW experiments, but it increases greatly at  $1.5\mu m$ .

## 5 Detection rates

Estimates of the coalescence rate of NS-NS binaries are performed in two main steps. Firstly, the merging rate in our Galaxy is evaluated and then, by assuming that this value is typical, extrapolations to the local universe are performed under the assumption of some adequate scaling. The galactic rate has been estimated by different authors and ranges from  $10^{-6}/yr^{-1}$  up to few times  $10^{-5}/yr^{-1}$ , but values as high as  $(2 - 3) \times 10^{-4}/yr^{-1}$  have already been reported (Tutukov & Yungelson 1993; Lipunov 1997; Kalogera et al. 2004). Here we adopt the approach by de Freitas Pacheco (1997) and de Freitas Pacheco et al. (2004).

Let us suppose a massive binary (masses of the components higher than  $9 M_\odot$ ) formed at the instant  $t'$ . Let  $\tau_*$  be the mean evolutionary timescale for the system to evolve into two neutron stars, typically of the order of  $10^8$  yr. Define  $P(\tau)$  as the probability per unit of time for a newly formed NS-NS binary to coalesce in a timescale  $\tau$  and define  $R_*(t)$  as the star formation rate (in  $M_\odot yr^{-1}$ ). Then, the galactic coalescence rate at instant  $t$  is

$$\nu_c(t) = f_b \beta_{ns} \lambda \int_{\tau_0}^{(t-\tau_*-\tau_0)} P(\tau) R_*(t - \tau_* - \tau_0) d\tau \quad (9)$$

D (Mpc)	Event rate $yr^{-1}$
10	$8.14 \times 10^{-3}$
15	$4.76 \times 10^{-2}$
20	$7.13 \times 10^{-2}$
30	$1.53 \times 10^{-1}$
40	$2.87 \times 10^{-1}$
50	$5.21 \times 10^{-1}$
70	1.68
100	3.86
150	4.25
200	10.1
300	34.0

Tab. 1 Expected event rates as a function of distance

where  $f_b$  is the fraction of massive binaries formed among all stars,  $\beta_{ns}$  is the fraction of formed binaries which remain bounded after the second supernova event and  $\lambda$  is the fraction of formed stars in the mass interval 9-40  $M_\odot$ . We have set  $\tau_0$  as the minimum timescale for a NS-NS binary to coalesce. Numerical simulations discussed in de Freitas Pacheco et al. (2004) allow the determination of  $\tau_0$ , the product  $f_b\beta_{ns}$  and the probability distribution  $P(\tau)$ . One obtains  $\tau_0 = 2 \times 10^5$  yr,  $P(\tau) \propto 1/\tau$  and  $f_b\beta_{ns} = 0.00432$ . This latter value corresponds to a natal kick velocity dispersion of about 230 km/s. If we adopt the galactic star formation history derived by Rocha-Pinto et al. (2000), it results for the present galactic NS-NS coalescence rate  $\nu_S = (4.1 \pm 2.0) \times 10^{-5} \text{ yr}^{-1}$ , where the estimated uncertainty is essentially due to uncertainties in the natal kick velocity dispersion and in the actual ratio between the number of single to binary pulsars derived from simulations. A similar calculation for a typical elliptical galaxy with an absolute magnitude  $M_B = -20.7$  gives a coalescence rate  $\nu_E = 2.1 \times 10^{-4} \text{ yr}^{-1}$  (de Freitas Pacheco et al. 2004). The weighted local coalescence rate was obtained assuming a fraction of 65% of spirals and 35% of ellipticals and lenticulars (S0's) and an elliptical-to-spiral luminosity ratio of 1.26. The resulting rate is  $\nu_c = 8.3 \times 10^{-5} \text{ yr}^{-1}$ .

Extrapolation from the local coalescence rate to the expected rate within a spherical volume of radius  $D$  probed by the detector is made through the scale factor  $K_B(D)$ . This factor is defined as the ratio between the total blue luminosity within the considered volume and the Milk Way luminosity. We use here the scale factor computed by de Freitas Pacheco et al. (2004), who considered the distribution of galaxies derived from the LEDA databasis and included the contribution of the Great Attractor, centered at the Norma cluster. The expected rates as a function of distance are given in *Tab. 1*.

The actual specifications on the VIRGO sensitivity show that an S/N of 7 is achieved at 13.6 Mpc for neutron stars binaries. An improvement of a factor 2.5 in S/N would allow VIRGO to explore with an S/N equal to 7 the universe up to 34 Mpc and bring VIRGO to a detection roughly every five years. A larger improvement of a factor 8 in S/N would reach a distance of 108 Mpc and four detections a year, *tab. 2*.

Noise reduction factor (c) band	Detection rate $\text{yr}^{-1}$	S/N = 7 at distance (Mpc)
1	$3.65 \times 10^{-2}$	13.6
3	$2.07 \times 10^{-1}$	34
10	3.99	108

*Tab. 2 Expected detection rates for actual and improved VIRGO*

## 6 Conclusions

We have determined the gain in S/N whenever the noise in VIRGO would be reduced in a chosen bandwidth and confirmed that mirror thermal noise, 42-140 Hz bandwidth, should be preferentially chosen for the R&D of advanced VIRGO for coalescing binaries detection. In such band, also thermal pendulum and shot noises should be reduced if large gains in S/N are to be achieved. We have calculated the detection rate at several distances an adequate S/N would reach. An optimized S/N would provide few detection events per year.

## 7 Acknowledgments

This research work was supported by the European Space Agency ESA with a G. Colombo Senior Research Fellowship to A. Spallicci; A. Brillat and J.-Y. Vinet are acknowledged for discussions.

## References

- Bondu F., Hello P. and Vinet J.-Y., 1998. VIR-NOT-LAS-1390-108.
- Braginsky V.B., Gorodetsky M.L. and Vyatchanin S.P., 1999. Phys. Lett. A, **264**, 1.
- Braginsky V.B. and Vyatchanin S.P., 2003. Phys. Lett. A, **312**, 244.
- de Freitas Pacheco J.A., 1997. Astrop. Phys., **8**, 21.
- de Freitas Pacheco, Regimbau T., Vincent S., Sathyaprakash B. and Spallicci A., 2004. To be submitted to Mon. N. Roy. Soc.

Harry G.M., Gretarsson A.M., Saulson P.R., Kittelberger S.E., Penn S.D., Startin W.J., Rowan S., Fejer M.M., Crooks D.R.M., Cagnoli G., Hough J. and Nagawaka N., 2002. *Class. Quant. Grav.*, **19**, 897.

Helström C.W., 1968. *Statistical theory of signal detection* (London: Pergamon).

Kalogera V., Kim C., Lorimer D.R., Burgay M., D'Amico N., Possenti A., Manchester R.N., Lyne A.G., Joshi B.C., McLaughlin M.A., Kramer M., Sarkisian J.M. and Camilo F., 2004. *Astrophys. J.*, **601**, L179.

Lipunov V.M., Postnov K.A. and Prokhorov M.E., 1997. *Mon. Not. R. Astron. Soc.*, **288**, 245.

Peters P.C., 1964. *Phys. Rev.*, **136**, 1124.

Peters P.C. and Mathews J., 1963. *Phys. Rev.*, **131**, 435.

Punturo M., 2003. VIR-NOT-PER-1390-51.

Rocha-Pinto H.J., Scalo J., Maciel W.J. and Flynn C., 2000. *AP. J.*, **531**, L115.

Schutz B.F., 1986. *Nature*, **323**, 310.

Spallicci A., 2003. VIR-NOT-OCA-1390-257.

Spallicci A., Królak A. and Frossati G., 1997. *Class. Quantum Grav.*, **14**, 577.

Tutukov A.V. and Yungelson L.R., 1993. *Mon. Not. R. Astron. Soc.*, **260**, 675.

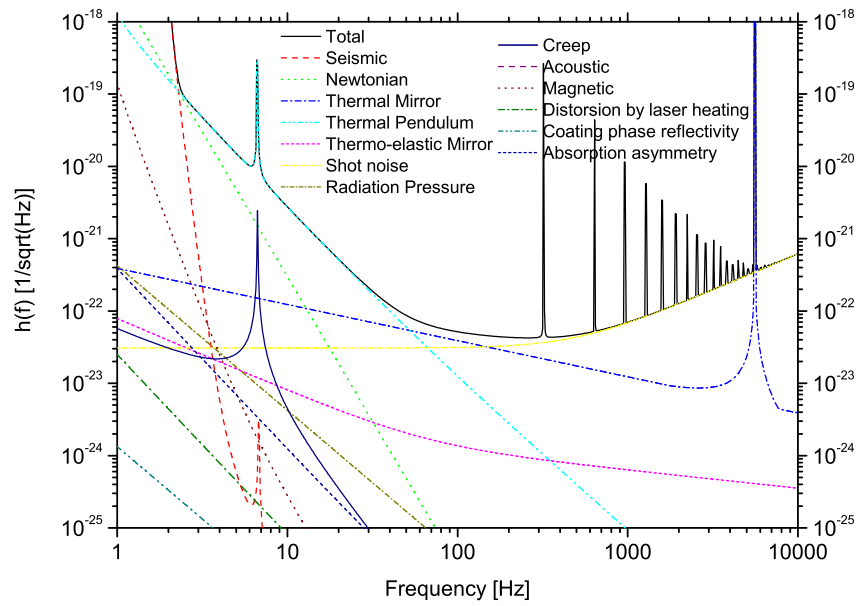


Figure 1: VIRGO strain sensitivity  $h(f)/\sqrt{Hz}$ . The noise spectral density  $I_{old}$  is the square of the strain sensitivity.

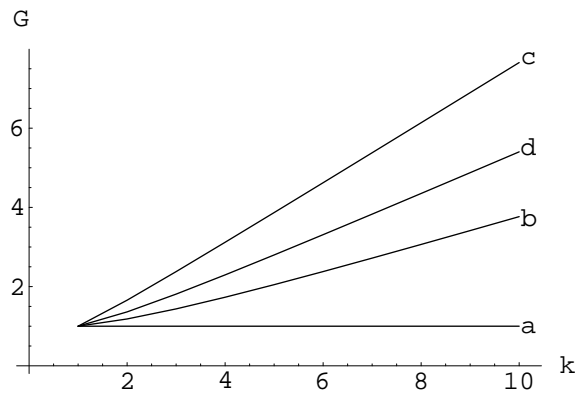


Figure 2: Gain  $G$  versus abatement of noise  $k$  for the four sub-bands a-d.

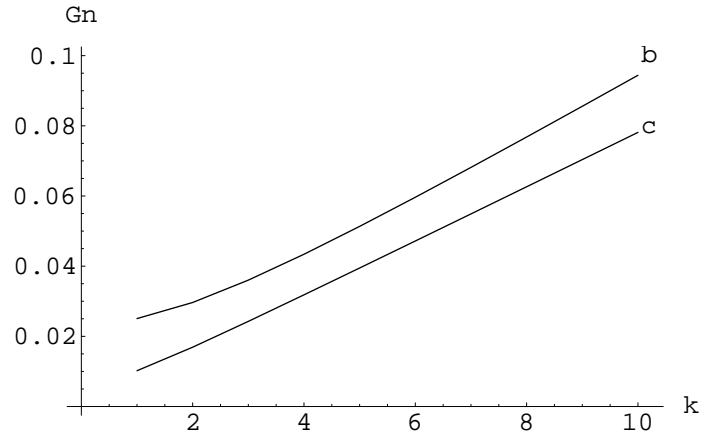


Figure 3: Normalized gain  $G$  versus abatement of noise  $k$  for the  $b, c$  sub-bands.

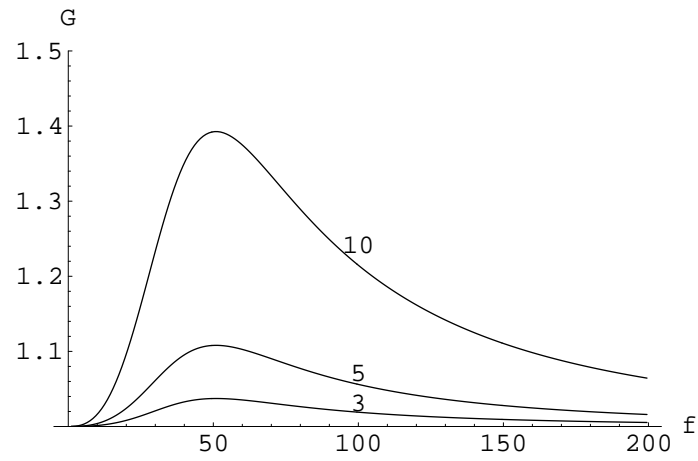


Figure 4: Gain  $G$  in the frequency range 1-200 Hz for three levels of abatement of noise ( $k = 3, 5, 10$ ), relative to an improvement in a bandwidth of 1 Hz.

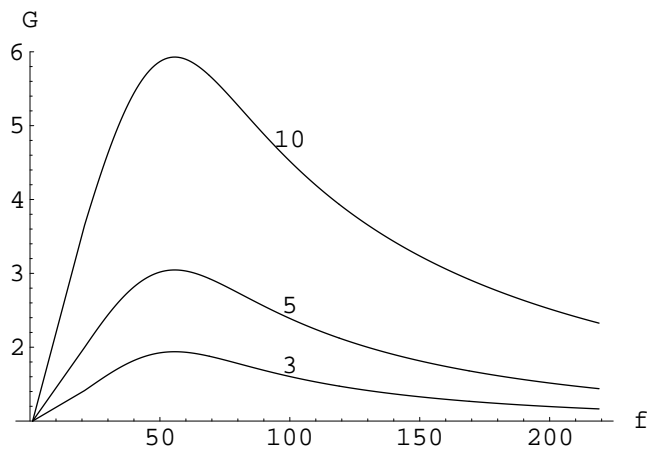


Figure 5: Gain  $G$  in the frequency range 1-200 Hz for three levels of abatement of noise ( $k = 3, 5, 10$ ), relative to an improvement in a bandwidth of 40 Hz.



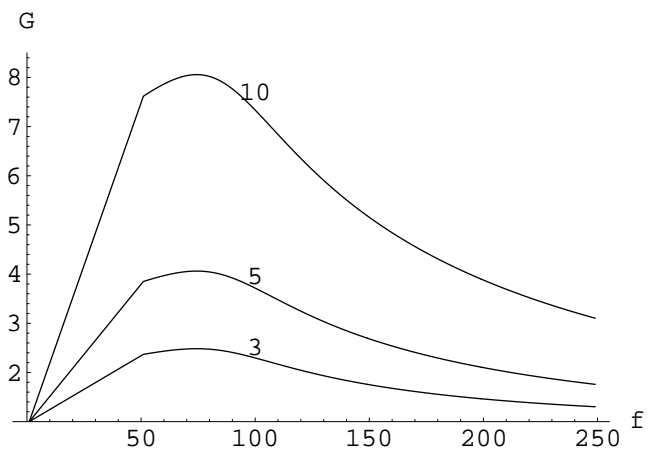


Figure 6: Gain  $G$  in the frequency range 1-200 Hz for three levels of abatement of noise ( $k = 3, 5, 10$ ), relative to an improvement in a bandwidth of 100 Hz.